ANGPTL7 and Its Role in IOP and Glaucoma

Suzette Farber-Katz Brown,[1] Hien Nguyen,[1] Philip Mzyk,[2] Michael L. De Ieso,[2] Andrea M. Unser,[3] Ian Brown,[1] Pujhitha Ramesh,[3] Hira Afzaal,[3] Feryan Ahmed,[3] Karen Y. Torrejon,[3] Alan Nhan,[4] Dalton Markrush,[4] Tom Daly,[4] Ellie Knecht,[4] William McConaughy,[4] Sara Halmos,[4] Zhiquan Lucy Liu,[4] Rachel Rennard,[4] Andrew Peterson,[1] and W. Daniel Stamer[2]

[1]Broadwing Bio, Waltham, Massachusetts, United States
[2]Duke University, Durham, North Carolina, United States
[3]Humonix Biosciences, Albany, New York, United States
[4]Alloy Therapeutics, Waltham, Massachusetts, United States

Correspondence: Suzette Farber-Katz Brown, Broadwing Bio, 275 2nd Ave STE 200, Waltham, MA 02451, USA; suzettebrownphd@gmail.com.
W. Daniel Stamer, Duke University, DUMC 3802, Durham, NC 27710, USA;
william.stamer@duke.edu.

Received: October 6, 2023
Accepted: February 14, 2024
Published: March 18, 2024

Citation: Brown SFK, Nguyen H, Mzyk P, et al. ANGPTL7 and its role in IOP and glaucoma. *Invest Ophthalmol Vis Sci.* 2024;65(3):22. https://doi.org/10.1167/iovs.65.3.22

Purpose. Loss-of-function variants in the *ANGPTL7* gene are associated with protection from glaucoma and reduced intraocular pressure (IOP). We investigated the role of ANGPTL7 in IOP homeostasis and its potential as a target for glaucoma therapeutics.

Methods. IOP, outflow facility, and outflow tissue morphology of *Angptl7* knockout (KO) mice were assessed with and without dexamethasone (Dex). ANGPTL7 was quantified in conditioned media from human trabecular meshwork cells in response to Dex, in effluent from perfused human donor eyes, and in aqueous humor from human patients treated with steroids. Antibodies to ANGPTL7 were generated and tested in three-dimensional (3D) culture of outflow cells and perfused human donor eyes. Rabbits were injected intravitreally with a neutralizing antibody targeting ANGPTL7, and IOP was measured.

Results. IOP was significantly elevated, but outflow facility and outflow tissue morphology were not different between *Angptl7* KO mice and littermates. When challenged with Dex, IOP increased in wild-type but not *Angptl7* KO mice. In human samples, increased ANGPTL7 was seen in the aqueous humor of patients treated with steroids, regardless of glaucoma status. Using 3D culture, recombinant ANGPTL7 decreased, and ANGPTL7-blocking antibodies increased hydraulic conductivity. Significantly, outflow facility increased in human eyes treated ex vivo with ANGPTL7-blocking antibodies, and IOP decreased for 21 days in rabbits after a single injection of blocking antibodies.

Conclusions. Using multiple models, we have demonstrated that excess ANGPTL7 increases outflow resistance and IOP and that neutralizing ANGPTL7 has beneficial effects in both naïve and steroid-induced hypertensive eyes, thus motivating the development of ANGPTL7-targeting therapeutics for the treatment of glaucoma.

Keywords: ANGPTL7, glaucoma, steroid-induced glaucoma, aqueous outflow, corticosteroids

Glaucoma is a leading cause of blindness worldwide[1] and is characterized by retinal ganglion cell degeneration, leading to optic nerve damage and ultimately vision loss.[2] Ocular hypertension, which is the primary and only modifiable risk factor for glaucoma, is the result of dysfunction of trabecular meshwork (TM) and/or Schlemm's canal (SC) cells in the conventional outflow pathway, resulting in increased resistance to drainage of aqueous humor. Unfortunately, current first- and second-line standard-of-care treatments do not target cells of the conventional outflow pathway. Combined with poor adherence to therapies, intraocular pressure (IOP) is poorly managed in many patients, and there is a strong need for more efficacious, longer lasting therapies.

The ANGPTL7 protein is a promising therapeutic target for glaucoma due to its genetic association with lower IOP and reduced risk of developing glaucoma.[3] Loss-of-function *ANGPTL7* variants are associated with lower IOP and protection from multiple forms of glaucoma, including the most prevalent form, primary open-angle glaucoma (POAG). In line with these observations, ANGPTL7 is highly expressed in TM cells, the prominent cell type in the conventional outflow tract.[4–6] Variants that destabilize ANGPTL7 and decrease the secretion of ANGPTL7 are associated with reduced IOP,[7] and increased levels of secreted ANGPTL7 have been found in the aqueous humor of human patients with glaucoma compared to controls.[8] In addition, *ANGPTL7* gene expression has been shown to increase in response to stressors associated with glaucoma pathobiology, including the glucocorticoid dexamethasone (Dex) and transforming growth factor-β.[5,9,10] Together, these data point toward ANGPTL7 as a strong therapeutic target for glaucoma;

however, the roles of ANGPTL7 in normal ocular physiology and in the pathophysiology of glaucoma are only poorly understood.

ANGPTL7 is a member of the angiopoietin-like family, of which there are eight members with a variety of physiological and pathophysiological functions.[11] Interestingly, ANGPTL7 has no known receptor, and other angiopoietin-like isoforms function by orchestrating complex protein–protein interactions without using cell surface receptors. Additionally, Gur-Cohen and colleagues[12] identified a role for ANGPTL7 in the regulation of lymphatic cell dynamics, which may be relevant to conventional outflow function, as SC cells are lymphatic/blood vasculature hybrids that depend upon TM cells for trophic support. In this study, we expanded upon current knowledge of the role of ANGPTL7 in IOP regulation and glaucoma using five complementary model systems, and we identified, characterized, and tested possible anti-ANGPTL7 therapeutic antibodies for glaucoma.

Methods

Patient Selection

This study was approved by the Human Research Protection Program at the University of California, San Francisco (UCSF), and adhered to the tenets of the Declaration of Helsinki for research involving human subjects. Informed consent was obtained from all patients. Twenty control patients, 12 uveitis patients, 36 glaucoma patients (various types with a majority POAG), and 14 glaucoma patients treated with steroids (10 uveitic glaucoma, 4 patients taking steroids for other sources of inflammation) underwent various ocular procedures such as cataract surgery or pars plana vitrectomy at UCSF Medical Center and Zuckerberg San Francisco General Hospital and Trauma Center. Clinical data including demographics and prior medical and ocular history were extracted from the electronic patient record.

Human donor eyes were obtained from Miracles in Sight Eye Bank via Duke University's BioSight Core Service. Donor families were consented and eyes recovered by Miracles in Sight Eye Bank. Eyes were distributed by BioSight under Duke University's Institutional Review Board exemption protocol (#113746).

Aqueous Humor Sample Collection

Aqueous humor was collected via anterior chamber paracentesis for all patients. Paracentesis was performed using a 30-gauge needle before injection of any intraocular agents. Approximately 100 µL of aqueous humor was collected. Paracentesis was performed at the time of cataract or other surgery for patients. Aqueous samples were then labeled with a predetermined identification number. Vitreous samples were collected during vitrectomy surgery. Before fluid infusion was turned on, a non-dilute sample of vitreous was obtained with the vitreous cutter using 25- or 27-gauge vitrectomy. The samples were transported on dry ice and stored at −80°C until sample processing.

Whole Globe Ocular Perfusions

To monitor the release kinetics of ANGPTL7, we built a custom metabolic chamber for collecting effluent from perfused human donor eyes while measuring outflow facility.[13] Upon receipt of a pair of human donor eyes, we positioned each eye with pupils facing upward on each mount. We used a 0.5-mL syringe with 27-gauge needle to extract ~200 µL of aqueous humor from each eye. Aqueous humor was stored in labeled vials at −80°C. We then removed the syringe from the eye and recannulated the puncture with a larger 25-gauge needle, positioned under the iris and connected to a syringe pump. We perfused the eyes (n = 3 pairs) with DBG perfusion buffer (Dulbecco's phosphate buffered saline plus 5.5-mM glucose; Thermo Fisher Scientific, Waltham, MA, USA) with 1 mg/mL anhydrous glucose (MP Biomedicals, Irvine, CA, USA) for 4 hours at 2.5-µL/min constant flow while continuously recording pressure. Effluent was collected at 2, 3, and 4 hours and immediately stored in labeled vials at −80°C. After 4 hours of perfusion, the TM tissue was carefully dissected from each eye and stored in labeled vials at −80°C.

To monitor the effect of anti-ANGPTL7 immunoglobulin G (IgG) on outflow facility, anterior chambers of human donor eyes (n = 6) were cannulated with two 25-gauge needles, one placed under the iris with the bevel facing up and connected to a pressure reservoir for maintaining constant pressure, and the other placed in the anterior chamber and connected to an exchange reservoir. We then perfused the eyes with DBG perfusion buffer for 60 minutes to allow for the eyes to acclimate and establish stable outflow facility at a constant pressure of 15 mmHg (while measuring flow over time). Perfusion was then halted, and one eye was exchanged with 5 mL of DBG perfusion buffer containing anti-ANGPTL7 IgG (40 µg/mL), and the other was exchanged with DBG perfusion buffer containing IgG isotype (40 µg/mL) as a control. Perfusion was restarted and continued with DBG perfusion buffer containing anti-ANGPTL7 IgG or the isotype IgG for 3 hours. After 3 hours, perfusion was stopped, and anterior chamber fluid from both eyes was exchanged with 5 mL of fixative (4% paraformaldehyde in PBS). The perfusion was then restarted, and the eyes were perfusion-fixed at 15 mmHg for 30 minutes, after which eyes were stored at 4°C overnight and switched to PBS the next day for long-term storage at 4°C.

Animals

Animals were handled in accordance with all applicable international, national, and institutional guidelines for the care and use of animals, including the National Institutes of Health Guide for the Care and Use of Laboratory Animals and the ARVO Statement for the Use of Animals in Ophthalmic and Vision Research. All procedures were approved by the Maze Therapeutics, Duke University, or Powered Research Institutional Animal Care and Use Committees.

Mice

Angptl7^{tm1Lex} is a knockout model for the gene *angiopoietin-like 7* (*Angptl7*) generated in a 129SvEv-C57BL/6 mixed genetic background (Taconic Biosciences, Germantown, NY, USA) (Supplementary Fig. S1A). *Angptl7*^{tm1Lex}, heterozygous (HET) littermates, and wild-type (WT) littermates used for these studies were 9 to 12 weeks of age upon study start and were allowed to acclimate to the facility for at least 7 days. The mice were housed in a 12-hour lights on/lights off cycle

Investigative Ophthalmology & Visual Science

at 7 AM and 7 PM. Food and water were provided ad libitum. Genotyping was performed at Taconic Biosciences using QIAGEN PCR reagents (QIAGEN, Germantown, MD) according to the manufacturer's recommended protocol using the following primers:

Forward primer	5′-GAGGTACAGCAGCAACAATA-3′
Reverse primer	5′-TGTTCCCCTTAGAGTCT-3′
Forward primer	5′-ACAATATTTAAGATGCTGCC-3′
Reverse primer (GT-IRES)	5′-CCCTAGGAATGCTCGTCAAGA-3′

WT mice generate a 208-bp PCR product, and KO mice generate a 296-bp product.

Verification of mouse knockout was performed in-house using quantitative PCR (qPCR) on mouse whole eye tissue. qPCR was performed using the TaqMan assays listed below on a ViiA 7 system (Thermo Fisher Scientific) according to the manufacturer's recommended protocol. The *Angptl7* TaqMan assay spans the exon 1–2 boundary.

Gene	TaqMan Catalog Number
Mouse *Angptl7*	Mm01256626_m1
Mouse *Gapdh* (housekeeping gene)	Mm99999915_g1

Mouse Tonometry

IOP measurements and outflow facilities and were taken for *Angptl7* KO, HET, and WT littermate mice, and the identity of genotypes was masked. IOP was measured with a TONOVET TV01 rebound tonometer (Icare, Vantaa, Finland) between 8 AM and 12 PM. Isoflurane was used to induce unconsciousness. Mice were placed on a platform in a nose cone and checked for lack of blinking response. The tonometer was placed about 4 mm away from the central cornea, making sure that the probe was in the horizontal position, and readings were recorded. The right eye (OD) is measured first and then the left eye (OS). Three measurements are taken per eye, and the average was calculated to determine OS/OD IOP.

Outflow Facility in Mice

Mice were euthanized, and the eyes were then enucleated and perfused with DBG perfusion buffer for 30 minutes at constant pressure (12 mmHg) to acclimate prior to the pressure step routine being run. Two mice were perfused per day (one KO and one WT), and the daily order of which genotype was perfused first was alternated. For each animal, facility measurements from each eye were averaged to produce one data point per animal (except where the measurement for one eye was excluded due to technical issues during the perfusion; thus, only one facility measurement was used for that animal). Thirty-two eyes (16 from each genotype) were fixed by immersion in 4% paraformaldehyde at 4°C overnight and then transferred into PBS and stored at 4°C.

Dex Osmotic Pump Model

Osmotic pumps (ALZet 1004; DURECT Corporation, Cupertino, CA, USA) were sterile-filled with either PBS or dexamethasone–cyclodextran solution (Sigma-Aldrich, St. Louis, MO, USA) for a dose of 4 mg/kg/d for the average 30-g mouse. The pumps were then left in 0.9% normal saline at 37°C for 48 hours before implantation. On day 0, body weight and IOP measurements were taken and then used to randomize treatment groups. Animals were anesthetized using isoflurane in an induction chamber and maintained on a nose cone (2%–3% isoflurane, 1 L/min oxygen) for the implantation. Loss of consciousness was determined by breathing pattern and toe pinch. A dose of carprofen (Rimadyl; Zoeitis, Parsippany, NJ, USA) was provided before making the incision. When the animals were deeply anesthetized, the back of the neck was shaved and cleaned with alternating swabs of 70% isopropyl alcohol and betadine. A small incision was made with a pair of sterile surgical scissors in the shaved area. Using a pair of sterile hemostats, a small pocket was made by opening and closing the hemostat in the subcutaneous space. The prefilled mini pump was inserted into the pocket, and the incision site was closed with wound clips. The stapled area of the skin was cleaned with a cotton tip applicator, and betadine was applied. Mice were then placed back in their cages with a heating pad to recover.

Mouse Histopathology

A single perfused eye from each of three WT and three *Angptl7* KO mice was fixed in 4% paraformaldehyde overnight and stored at 4°C in PBS. The anterior segment from each eye was isolated, and each segment was divided into four quarters. Two quarters from each eye (totaling 12 quarters) were prepared in plastic-embedded semi-thin sections stained with methylene blue for visualization of the outflow tissues, including the trabecular meshwork, Schlemm's canal, and distal vasculature.

Mouse Cornea Measurements

Semi-thin plastic sections were made from either WT or *Angptl7* KO mouse eyes ($n = 3$ eyes per group). All imaging and measurements were performed utilizing a confocal microscope and Nikon Elements software. For each eye, sections were imaged with white light by tile scanning to ensure that consistent images were generated. From each tile scan, individual sections were measured by tracing along the cornea for 1 mm starting from the outer sulcus of the limbus to maintain consistent spacing across all sections. Cornea measurements were then recorded perpendicular to this point on each section measured.

Rabbits

Male New Zealand White rabbits at 4 to 6 months of age on arrival were single-housed in a 12-hour light/12-hour dark facility. Food and water were provided ad libitum. Animals underwent a pre-shipment ocular assessment by the vendor. An acclimation period of 7 days was allowed between animal receipt and the start of treatment to adapt the animals to the laboratory environment. One rabbit was removed on day 18 out of an abundance of caution due to slight squinting of the OD eye.

Intravitreal Dosing

On day 0, prior to dosing, animals were dilated with 1% tropicamide HCl and then given buprenorphine, 0.01 to 0.05 mg/kg, subcutaneously. Animals were then tranquilized for the injections (ketamine/xylazine 50/10 mg/kg

Investigative Ophthalmology & Visual Science

intramuscularly), and the eyes were aseptically prepared using topical 5% betadine solution, followed by rinsing with sterile eye wash and the application of one drop of 0.5% proparacaine HCl. The conjunctiva was gently grasped with Colibri forceps, and the injection was made using a 27- to 30-gauge needle, 2 to 3 mm posterior to the superior limbus (through the pars plana), with the needle pointing slightly posteriorly to avoid contact with the lens. Animals were injected with 50 µL antibody buffer (10-mM histidine HCl, 10% α,α-trehalose dehydrate, and 0.01% polysorbate 20, pH 5.5) or 40 mg/mL anti-ANGPTL7 antibody (in same antibody buffer). After the syringe contents were dispensed, the needle was held in place for approximately 5 seconds and then slowly withdrawn. Following the injection procedure, one drop of antibiotic ophthalmic solution was applied topically to the ocular surface, and animals were allowed to recover normally from the procedure.

Rabbit Tonometry

IOP was measured in both eyes of all animals between 5 AM and 8 AM. The measurements were taken using a TONOVET probe (Icare) without the use of topical anesthetic. The tip of the TONOVET probe was directed to gently contact the central cornea. Six consecutive measurements were obtained. After the sixth measurement, the average IOP shown on the display was recorded. Animals were not tranquilized for the procedure.

Cell Culture

Human trabecular meshwork (HTM) cells were isolated from postmortem donor eyes and cultured and characterized according to established protocols.[14,15] The HTM cells were cultured in low-glucose Dulbecco's Modified Eagle Medium (DMEM) with Gibco GlutaMAX (Thermo Fisher Scientific) supplemented with 10% fetal bovine serum (FBS; R&D Systems, Minneapolis, MN, USA) and Gibco 1% penicillin–streptomycin (Thermo Fisher Scientific). Cells were grown at 37°C with 5% CO_2 in a humidified chamber. For experiments, cells underwent a differentiation step for at least 1 week in 1% FBS, as described previously.[16] Cells were not used past passage 6.

qPCR on Human Cells

Cells were harvested using a Cells-to-C_T kit (Thermo Fisher Scientific) according to the manufacturer's recommended protocol. cDNA was prepped using the kit, and qPCR was run using the TaqMan assays listed below on the ViiA 7 system according to the manufacturer's recommended protocol.

Gene	TaqMan Catalog Number
ANGPTL7	Hs00221727_m1
GAPDH (housekeeping gene)	Hs99999905_m1

ANGPTL7 ELISA

ELISA plates containing 384 wells were coated with 30 µL of 500-ng/mL anti-human ANGPTL7 (hANGPTL7) IgG capture antibody (Broadwing Bio, San Francisco, CA, USA) in coating buffer (10× coating buffer, pH 9.6, diluted to 1× in water; Boca Scientific, Dedham, MA, USA) and incubated overnight at 4°C. Plates were then blocked with 100 µL 1% BSA in PBS with 0.05% Tween 20 (BSA/PBST) and stored at 4°C for at least 24 hours. Samples were diluted 1:10 in 1% BSA/PBST, and 20 µL of each sample was added to the precoated wells of the plates. Samples and standards (ANGPTL7 recombinant protein; Broadwing Bio) were incubated at 4°C overnight. After incubation, the plates were washed in PBST using an automated plate washer, and 30 µL of 200-ng/mL biotinylated anti-hANGPTL7 detection antibody (Broadwing Bio) was added to the treated wells, followed by an incubation for 1 hour at room temperature, with shaking. Pierce Streptavidin-HRP (Thermo Fisher Scientific) was added after the plates were washed with PBST, and the plates were incubated for 1 hour at room temperature in the dark. The plates were washed with PBST for a final time, and 3,3′,5,5′-tetramethylbenzidine (TMB) substrate (Pierce TMB Substrate Kit; Thermo Fisher Scientific) was added to develop the plates. After 15 to 30 minutes, 2-M sulfuric acid was added to stop the reaction. Plates were read using a plate reader at a wavelength of 450 nm. Samples were calibrated against ANGPTL7 recombinant protein, and samples below the lower limit of quantitation (LLOQ) were reported as LLOQ/2 or 0.32 ng/mL. Similar protein levels were seen with our ELISA compared to a commercially available ANGPTL7 ELISA (RayBiotech, Peachtree Corners, GA, USA). The Broadwing antibodies demonstrated specificity for the human ANGPTL7 protein, as they did not elicit a signal in human serum, and negligible levels were seen in vitreous and aqueous humor from other species (monkey and rabbit).

Conventional Outflow Facility Using the Humonix Biosciences Three-Dimensional HTM/Human Schlemm's Canal Tissue Model

Methods have been described in Bastia et al.[17] Briefly, primary HTM cells were isolated from three healthy donor tissue rings discarded after penetrating keratoplasty (Cell Applications, San Diego, CA, USA). The cells were plated in 1% gelatin-coated, 75-cm^2 cell culture flasks and cultured in modified Improved Minimum Essential Medium (IMEM; Thermo Fisher Scientific) containing 10% premium select heat-inactivated FBS (Atlanta Biologicals, Lawrenceville, GA, USA) and 0.1-mg/mL gentamicin (Thermo Fisher Scientific). Fresh culture medium was supplied every 48 hours, and cells were maintained in a humidified atmosphere with 5% carbon dioxide until confluence. HTM cells were then trypsinized using 0.25% trypsin/0.5-mM EDTA (Thermo Fisher Scientific), subcultured onto 1% gelatin-coated microporous scaffolds attached to aluminum rings, and placed in 24-well plates. The HTM cells were seeded at a density of 40,000 to 50,000 cells per scaffold. Then, primary human Schlemm's canal (HSC) cells from two donors (provided by The Stamer Lab, Duke University Durham, NC, USA) were plated in 75-cm^2 cell culture flasks with 10% premium select FBS (Atlanta Biologicals) in DMEM (Life Technologies, Carlsbad, CA) supplemented with penicillin (100 units/mL), streptomycin (0.1 mg/mL), and L-glutamine (0.292 mg/mL) (Sigma-Aldrich). The cells were maintained at 37°C in a humidified atmosphere with 5% CO_2, with fresh medium being replaced every 48 hours until confluence. When confluent, the HTM constructs were inverted, and primary HSC cells (40,000–50,000 cells/sample) were cultured on the other side of the

scaffold for 7 to 10 days. After the three-dimensional (3D)-HTM/HSC constructs reached confluency, they were serum starved (1% FBS–DMEM) for 1 day before treatment with vehicle, Dex (500 nM), or ANGPTL7 with or without blocking antibodies for 9 days followed by perfusion studies. The 3D-HTM/HSC constructs were perfused with high-glucose (4.5 g/L) DMEM (Thermo Fisher Scientific) supplemented with gentamicin. Perfusion medium flowed from the apical-to-basal direction across the TM cells, then across the SC cells from the basal-to-apical direction, as the basal side of the TM crosstalks with the basal side of the SC cells. The temperature was maintained at 34°C throughout the experiment with pressure continuously monitored and recorded. After perfusion, the hydraulic conductivity (outflow facility) of the constructs was calculated from the inverse of the slope of the pressure versus flow per unit surface area.

Biomimetic Scaffold Fabrication

SU-8 2010 (MicroChem Corp., Newton, MA) was used to develop freestanding biomimetic porous microstructures that served as scaffolds on which primary HTM cells were cultured. Scaffolds were fabricated using standard photolithographic techniques as previously described.[18] Briefly, a release layer was spin-coated on the wafer and baked at 150°C. SU-8 2010 was applied by spin-coating to a final thickness of 5 mm; the wafer was then baked at 95°C and cooled to room temperature. The resist was ultraviolet (UV)-exposed through a mask containing the desired pattern, baked at 95°C, and developed in propylene glycol methyl ether acetate developer (MicroChem Corp.) SU-8 scaffolds with the desired features were released from the substrate, washed with acetone, and sterilized using 70% ethanol. After the ethanol dried, the scaffolds were placed under UV light for 1 hour per side; they were then coated with 1% gelatin on both sides and allowed to dry.

Antibody Generation

ANGPTL7 Immunization

Four cohorts of Alloy Therapeutics (Waltham, MA, USA) transgenic humanized mice, ATX-GK, were immunized with various human ANGPTL7 antigens using the standard 5-week repetitive immunization at multiple sites (RIMMS) protocol: 10 µg subcutaneous dosing of antigen emulsified in complete Freund's adjuvant followed by five weekly subcutaneous dosing of antigen emulsified in incomplete Freund's adjuvant.

- Cohort 1: Three ATX-GK mice immunized with human ANGPTL7 fibrinogen domain
- Cohort 2: Three ATX-GK mice immunized with full-length human ANGPTL7 monomeric variant L59P_L84P
- Cohort 3: Three ATX-GK mice immunized with full-length human ANGPTL7 monomeric variant L59 GGPGG
- Cohort 4: Three ATX-GK mice immunized with human WT ANGPTL7 multimer

Sample bleeds were taken at week 4 and tested for antigen-positive serum titer and purification tag-negative serum titer by ELISA. ELISA plates were coated with either 1 µg/mL of ANGPTL7 immunogen or an irrelevant protein with the same purification tag as the immunogen. Antigen-coated plates were incubated with seven 10-fold serial dilutions of sera starting at 1:300. Antibodies bound to antigen were detected by anti-mouse IgG horseradish peroxidase secondary antibody and one-step TMB solution. The absorbance signal at 450 nm was measured with an ELISA microplate reader.

Antibody Sequence Recovery

Hybridoma

Immune tissues from high-titer mice were harvested and preserved for antibody discovery. Hybridoma cell lines producing ANGPTL7 antibodies were produced by fusion of single B cells from the spleen and lymph nodes of titer-positive mice with SP2/0 myeloma cells. Twenty 96-well plates of hybridoma fusions were generated and expanded. Hybridomas expressing ANGPTL7-specific antibodies were detected by antigen binding by ELISA. The affinity of antibodies in the hybridoma supernatants was measured by surface plasmon resonance (SPR) using an Octet system (Octet HTX; ForteBio, Fremont, CA, USA). ANGPTL7 antibodies in hybridoma supernatant were loaded on a biosensor. Response was measured as a nanometer shift in the interference pattern and was proportional to the number of antibodies bound to the surface of the biosensor. The binding interaction of ANGPTL7 to the immobilized antibodies was measured as association (k_{on}). Following analyte association, the biosensor was dipped into PBS without ANGPTL7, and the bound antigen was allowed to dissociate from the antibody (k_{dis}). K_D (M), or affinity of the antibodies for ANGPTL7, was measured as k_{dis}/k_{on}.

Heavy and light chains from validated hybridomas were sequenced. RNA was isolated from ANGPTL7 antibody–secreting hybridomas, and heavy- and light-chain variable regions were cloned by reverse transcription using gene-specific primers followed by PCR amplification with variable chain gene-specific primers. PCR products were sequenced by standard Sanger sequencing methods.

Phage Display

Variable heavy and light chains were amplified from the spleens of high-titer immunized mice by reverse transcription using gene-specific primers followed by PCR amplification with variable chain gene-specific primers. Variable regions were cloned into a phage display vector designed to express Fabs on phage g3p protein. Libraries of phages expressing unique Fabs were amplified and purified. Phages were allowed to bind to biotinylated ANGPTL7 antigens captured on streptavidin magnetic beads. Phages remaining bound to antigen beads after several stringent washes were eluted using a basic triethylamine solution and neutralized with Tris buffer (pH 8.0). Eluted phages were reinfected into TG1 bacterial cells, amplified by co-infection with M13 helper phage, and purified by polyethylene glycol (PEG) precipitation. Purified phages expressing Fabs were selected for antigen binding as described. Phages from the second round were diluted and infected into TG1 cells. Polyclonal pools of phage output from two rounds of panning were tested by ELISA to confirm that the pools contained ANGPTL7-specific phages. Variable heavy- and light-chain regions were sequenced from single infected bacterial colonies using rolling circle amplification and standard Sanger sequencing.

Antibody Expression

Unique variable heavy- and light-chain pairs from hybridoma and phage display campaigns were cloned into vectors designed to express full-length antibodies as IgGs in HEK293 cells under the control of a HEK293/RFP (CMV) promoter. Antibody expression vectors were complexed with polyethylenimine and transfected into HEK293 cultures. After 5 days of shaking at 37°C in 293 cell culture media, antibodies were captured on agarose-based protein A resin. After several stringent washes, antibodies were eluted in glycine solution (pH 3), neutralized with HEPES (pH 9), and buffer exchanged into PBS.

Octet Kinetics

Binding experiments were performed on the Octet HTX in 1× PBS (pH 7.4), 0.1-mg/mL BSA, 0.05% sodium azide, and 0.02% Tween 20. To measure monovalent binding kinetics, antibodies at a concentration of 50 nM were loaded onto pre-hydrated Anti-Human IgG Fc Capture (AHC) biosensors (ForteBio) for 5 minutes. The loaded sensors were dipped into monovalent human ANGPTL7–His at a concentration ranging from 0.343 to 250 nM (a serial threefold dilution) for 5 minutes of association, followed by 10 minutes of dissociation. Results were analyzed with ForteBio Data Analysis 11.1 and fit globally to a 1:1 binding model to determine the monovalent K_D.

Octet Reactivity

Binding experiments were performed on the Octet HTX in 1× PBS (pH 7.4), 0.1 mg/mL BSA, 0.05% sodium azide, and 0.02% Tween 20. Antibodies at a concentration of 50 nM were loaded on pre-hydrated AHC biosensors for 5 minutes. The loaded sensors were dipped into monovalent human ANGPTL7–fibrinogen–His, human ANGPTL7–GGPGG_sub-His, or human ANGPTL7–FLAG multimer at concentrations of 200 nM, 100 nM, or 100 nM, respectively. The 5-minute association of ANGPTL7 proteins was followed by a 10-minute dissociation. Results were analyzed with ForteBio Data Analysis 11.1 and fit to a 1:1 binding model to determine the monovalent K_D. Responses (nm) at the end of the association were also included in the report.

Species reactivity was similarly evaluated on the Octet. Antibodies were immobilized on the AHC sensors as previously described. The loaded sensors were dipped into rabbit ANGPTL7–his (internally produced) or mouse ANGPTL7–His (R&D Systems) at a concentration of 200 nM for 5 minutes of association followed by a 10-minute dissociation. Results were analyzed with ForteBio Data Analysis 11.1 and fit to a 1:1 binding model to determine the monovalent K_D. Responses (nm) at the end of the association were also included in the report.

Epitope Binning

A high-throughput epitope binning experiment was performed on real-time label-free biosensors (Carterra LSA; Carterra, Salt Lake City, UT, USA) to sort the panel of mAbs into bins based on their ability to block one another for binding to human ANGTPL7. Antibodies were covalently printed on a HC200M chip (Carterra). The chip was activated with 33-mM sulfo-N-hydroxysuccinimide (sulfo-NHS) and 133-mM 1-ethyl-3-(3-dimethylaminopropyl)carbodiimide hydrochloride (EDC) in 100-mM 2-(N-morpholino) ethanesulfonic acid (MES) buffer (pH 5.5) for 7 minutes. Antibodies at 10 mg/mL in acetic acid buffer (pH 4.5) were used for printing for 10 minutes. The printed chip was then quenched with 1-M ethanolamine (pH 8.5) for 7 minutes. A running buffer of PBS (pH 7.4), 1% BSA, and 0.05% Tween 20 was used for the binning experiment. In a pairwise epitope binning analysis, human ANGPTL7 and antibody 2 (analyte antibody) were sequentially applied to the sensor chip covalently pre-loaded with antibody 1. An increase in response upon exposure to the analyte antibody indicates non-competition between the two antibodies, whereas a lack of change in the signal indicates competition. Antibodies having the same blocking profiles toward others in the test set were grouped into one bin. Community network plots were used to cluster mAbs that shared similar but not necessarily identical competition profiles.

Epitope Mapping

Epitopes were determined using previously published protocols for linear peptide arrays and discontinuous epitope mapping.[19,20] Briefly, these arrays contain immobilizing short overlapping peptide sequences in a grid pattern on a solid support to study protein interactions and functions. Alternatively, the Chemical Linkage of Peptides onto Scaffolds (CLIPS) technology was used to immobilize epitopes contained within loops, beta sheets, or helical structures. Samples are then tested for binding in an ELISA-like assay.

Statistics

The sample size of each experiment is displayed in the figures or in the corresponding figure legends. All statistical cutoffs were set at $P < 0.05$. To determine the statistical significance between IOPs and outflow facilities of WT/KO mice, unpaired *t*-tests were used. For WT/KO mouse corneal thickness measurements, an unpaired *t*-test was used. For experiments involving mice implanted with osmotic pumps, ANOVA with Tukey's multiple comparison test was used to determine statistical significance. For experiments using the 3D-HTM/HSC model, one-way ANOVA was used. For human aqueous humor samples, the Kruskal–Wallis test followed by Dunn's multiple comparison test was used. For human outflow facility experiments, a paired *t*-test was used. For the rabbit study, statistical significance was calculated using ANOVA with Sidak's multiple comparison test.

Results

Knockout of *Angptl7* Impaired the Dex-Induced IOP Increase

To investigate the role of ANGPTL7 in the regulation of IOP, we utilized *Angptl7*^{tm1Lex} mice, a global knockout on a mixed 129/SvEv-C57BL/6 background (Supplementary Figs. S1A, S1B). We measured baseline IOP in untreated KO or WT littermates. Surprisingly, the IOPs of the KO were significantly elevated compared to their WT littermates when measured at a California site (12.08 ± 0.22 vs. 11.18 ± 0.18, respectively; $P = 0.004$) (Fig. 1A). This elevated pattern was confirmed in littermates at a separate site (19.74 ± 0.75 vs. 18.63 ± 0.66, respectively; $P = 0.02$) (Supplementary Fig. S1C). Correspondingly, a small (~5%) but insignificant ($P = 0.14$) increase in corneal thickness was observed in KO mice (Supplemental Fig. S1D).

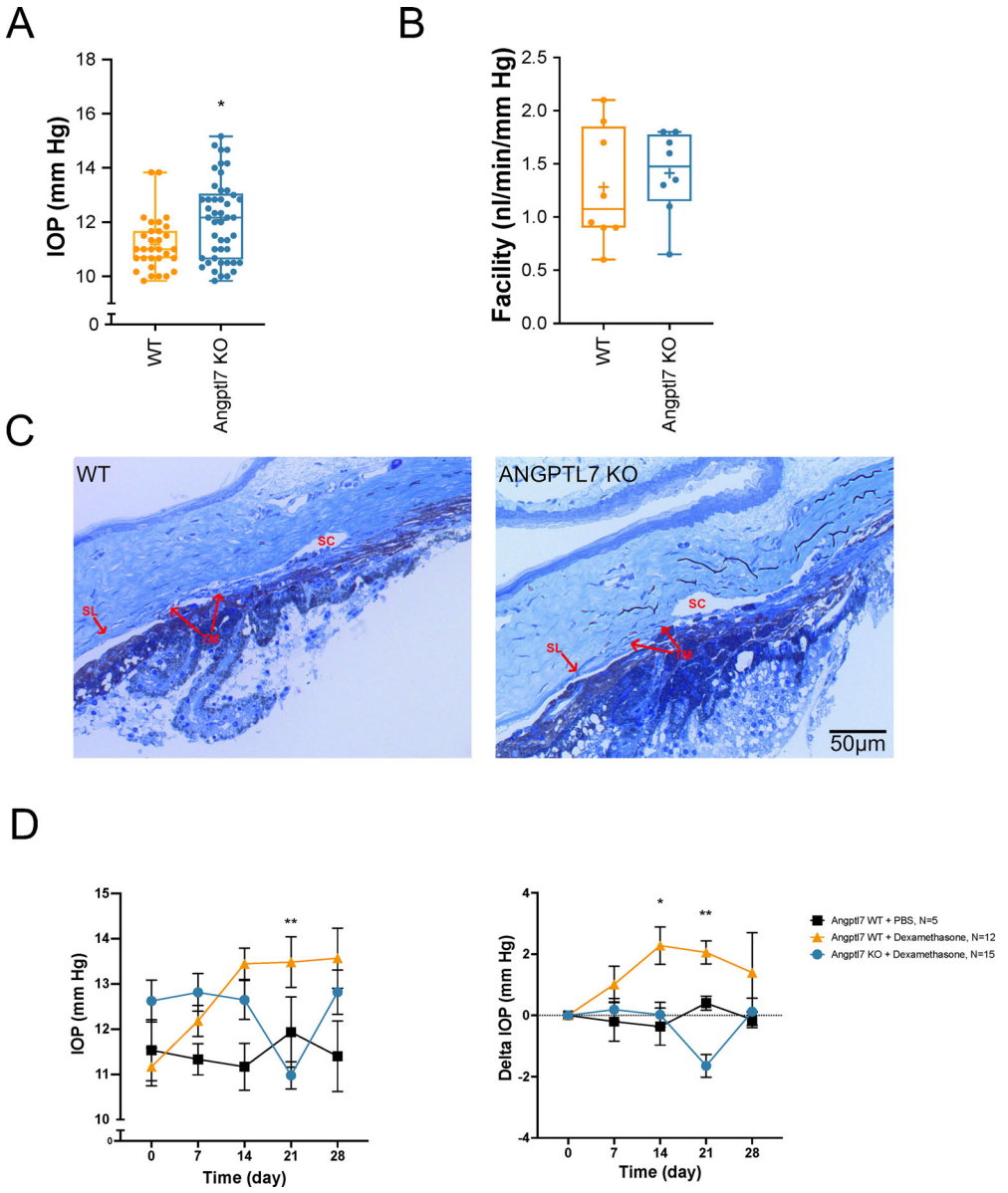

Figure 1. Effects of *Angptl7* deletion in mice. (**A**) KO of *Angptl7* in mice ($n = 46$) resulted in slightly higher IOP compared to WT littermates ($n = 31$), as quantified at a California site. Data are presented as box-and-whisker plots with a median line and mean represented by a + sign (*$P = 0.004$, unpaired *t*-test). (**B**) There was no significant difference in facility between *Angptl7* KO and WT ($n = 8$ mice each; not significant, unpaired *t*-test). Data are presented as box-and-whisker plots with a median line and mean represented by a + sign. (**C**) Representative images of a semi-thin section of iridocorneal angles. Shown is an image of a WT mouse iridocorneal angle (*left*) and an image of an *Angptl7* KO mouse iridocorneal angle (*right*). Scale is shown on *bottom right* of the ANGPTL7 image. TM, SC, and Schwalbe's line (SL) are demarcated. (**D**) WT or KO mouse littermates were implanted with Dex or vehicle (PBS) osmotic pumps. IOP was measured (*left*), and the change in IOP (normalized to time 0) was calculated (*right*) over 28 days. IOP increased with time in WT mice implanted with Dex osmotic pumps, whereas no increase was seen in *Angptl7* KO littermates also implanted with Dex osmotic pumps ($n \geq 5$; *$P < 0.05$ or **$P < 0.01$ WT vs. KO, ANOVA with Tukey's multiple comparison test). No difference in IOP over time was seen in mice implanted with control PBS osmotic pumps.

Facility was measured in WT and KO littermates, with no significant differences between the two groups (1.28 ± 0.19 vs. 1.41 ± 0.14 nL/min/mmHg, respectively) (Fig. 1B). These mouse eyes were fixed, and plastic-embedded semi-thin sections were stained with methylene blue for visualization of the outflow tissues, including the TM, SC, and distal vasculature. In the images examined, including the representative images shown in Figure 1C, the outflow tract appears similar in WT and KO eyes.

In parallel studies, WT and KO mice were implanted with an osmotic pump containing either Dex or PBS as a control. IOP was measured weekly over a total of 28 days. Although IOP increased as expected in the WT mice implanted with a Dex pump, the KO mice showed no increase in IOP (Fig. 1D). As observed previously,[21] there was a decrease in body weights in mice of both genotypes implanted with Dex pumps compared to control (Supplementary Fig. S1E), confirmation that the pumps were dispensing correctly.

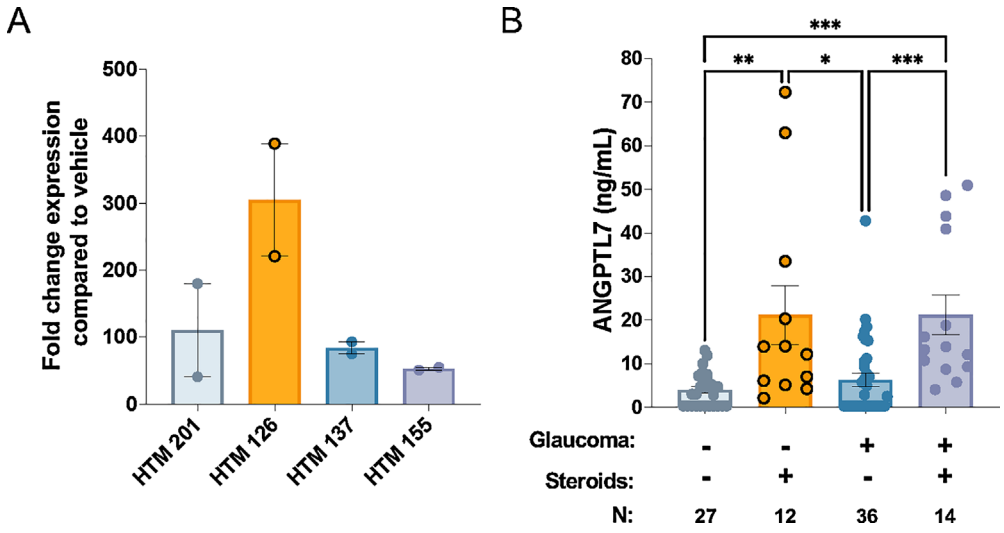

Figure 2. Human ANGPTL7 levels induced by steroid treatment. (**A**) HTM cells were treated with 100-nM Dex or ethanol vehicle for 5 days, and *ANGPTL7* gene expression was measured by qPCR. Expression of *ANGPTL7* in the presence of Dex was normalized to expression in the presence of vehicle. Data are shown as mean ± SEM ($n = 2$ or 3). (**B**) Human ANGPTL7 was quantified in aqueous humor samples using ELISA (*$P < 0.05$, **$P < 0.01$, ***$P < 0.001$, Kruskal–Wallis test followed by Dunn's multiple comparison test). Control and glaucoma samples without steroids were not statistically different (Kruskal–Wallis test followed by Dunn's multiple comparison test). Samples below the limit of quantitation (LOQ) are entered as 0.5× the LOQ (0.32 ng/mL). Data are shown as mean ± SEM.

ANGPTL7 Was Elevated Following Treatment With Steroids

To examine the effects of Dex on TM cells specifically, additional experiments were performed using human cells and tissues. Primary HTM cells were cultured on plastic to generate a monolayer of cells that subsequently underwent a differentiation step in 1% serum for at least 1 week. Cells were then treated with Dex or EtOH (vehicle control) for 5 days. Supernatant was collected for ELISA quantification, and the cells were harvested for qPCR. Large increases in both *ANGPTL7* gene expression and ANGPTL7 protein secretion were induced by Dex (Fig. 2A, Supplementary Figs. S2A, S2B). ANGPTL7 secretion by cells treated with vehicle was minimal (<2 ng/mL) (Supplementary Figs. S2A, S2B). To determine whether these results mirrored what is seen in patients, we quantified ANGPTL7 levels using ELISA in human aqueous humor samples that were obtained from consented patients undergoing various procedures such as cataract surgery. Details of the patient cohort are described in Supplementary Table S1. The steroid treatment is shown as bold in the table. ANGPTL7 levels were quantified in control patients, uveitis patients treated with steroids, glaucoma patients not treated with steroids, and glaucoma/uveitic glaucoma patients treated with steroids. Mirroring the results with TM cells in culture, ANGPTL7 levels were significantly elevated in all patients receiving steroid treatment, regardless of glaucoma status (Fig. 2B). Therefore, the steroid effect translates from primary cells to the human eye.

ANGPTL7 Antibody Discovery and Screening

ANGPTL7 antibodies were generated by both the hybridoma and phage techniques. Cross-blocking groups and general binding region (fibrinogen or coiled-coil domain) were determined (Fig. 3A). Binding to human, rabbit, pig, mouse, and monkey proteins was verified (Supplementary Table S2). Epitope mapping was performed for ANGPTL7 antibody 1 (AAb-1), and the majority of binding occurred in the globular fibrinogen domain (Fig. 3B).

To test the functionality of candidate ANGPTL7 antibodies, we developed a screening assay for hydraulic conductivity (outflow facility) of bioengineered 3D-HTM/HSC. The assay was validated with three HTM cell strains, in which Dex reduced outflow facility (Fig. 4A). With increasing concentration of recombinant ANGPTL7 (0.56–3.3 nM), outflow facility decreased in each of the three cell strains. Strain 2 was selected for further studies due to its superior response to recombinant ANGPTL7. Seventeen different monoclonal anti-ANGPTL7 IgGs (AAb-1–AAb-17) were screened in this bioengineered 3D-HTM/HSC model at 10× molar excess (11-nM antibody with 1.1-nM ANGPTL7), and the top six antibodies significantly rescued outflow facility effects of ANGPTL7 alone (Fig. 4B).

ANGPTL7 Antibodies Lowered IOP In Vivo

To establish the concentration of anti-ANGPTL7 IgGs that would likely be needed for therapeutic purposes, we devised a method to quantify ANGPTL7 secretion from the TM of perfused human eyes ex vivo. Donor eye demographic data are provided in Supplementary Table S3. A custom metabolic chamber was built to collect effluent from perfused human donor eyes ($n = 3$ pairs for 4 hours at 2.5-µL/min constant flow). ANGPTL7 levels were dramatically higher in the effluent (446 ± 55 ng/mL, ~10 nM; three patients, six eyes, six effluent collections per patient) compared to the aqueous humor (64 ± 12 ng/mL, ~1.4 nM; $P = 0.0002$) (Fig. 5A), which was collected prior to perfusion. To assess the eye viability, facility was measured and found to be in the normal range with no significant differences between the right and left eyes (Supplementary Fig.

Investigative Ophthalmology & Visual Science

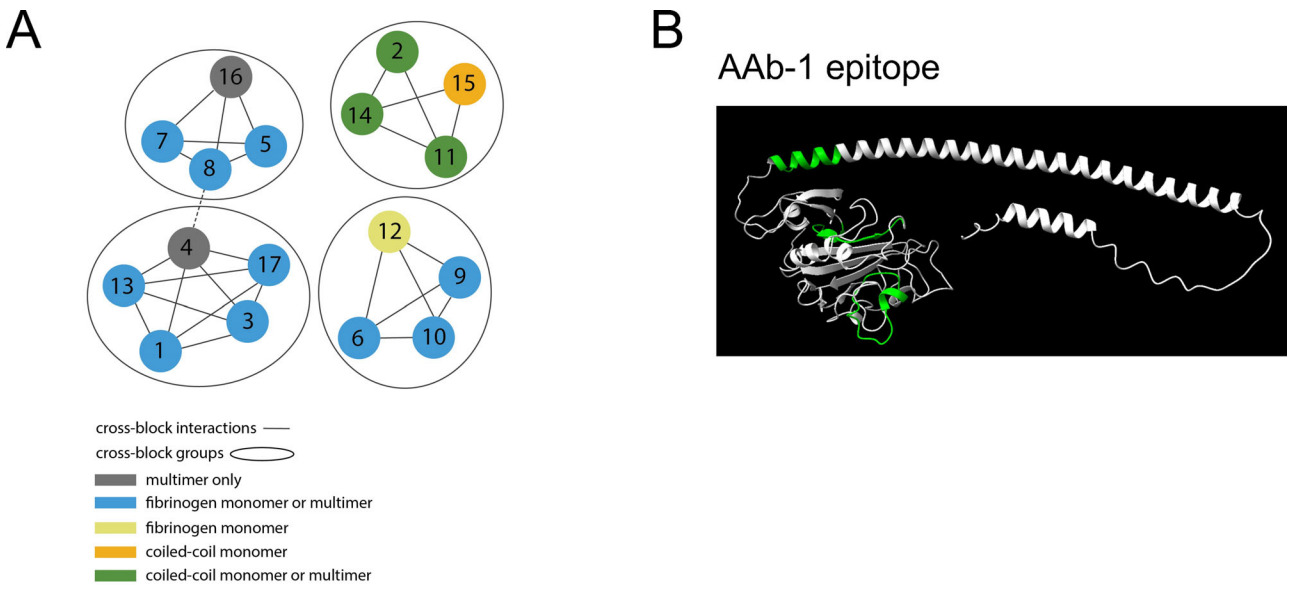

Figure 3. Antibody characterization. (**A**) Schematic of four antibody cross-block groups for 17 antibodies. (**B**) Epitope of AAb-1 shown in *green* on ANGPTL7 protein.

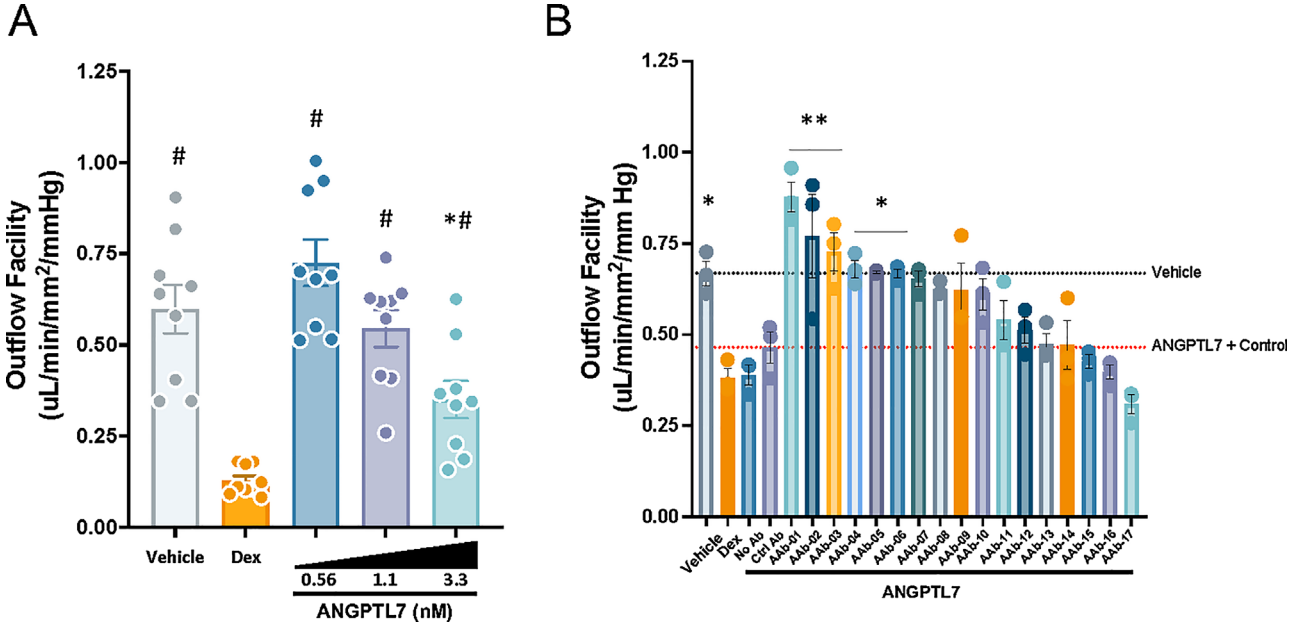

Figure 4. Assay for effects of ANGPTL7 or anti-ANGPTL7 on outflow facility. (**A**) A dose-responsive decrease in outflow facility was seen in the bioengineered 3D-HTM/HSC tissue model at concentrations of 0.56, 1.1, and 3.3 nM of recombinant ANGPTL7 (25, 50, and 150 ng/mL, respectively; $n = 3$ donors, run in triplicate; $^{*}P < 0.05$ vs. vehicle control; $^{\#}P < 0.05$ vs. Dex, one-way ANOVA with Tukey's multiple comparison test). (**B**) Donor 2 was selected for its superior response to ANGPTL7 at 1.1 nM. Antibodies were added at 10× molar excess at 11 nM. Both Dex and ANGPTL7 reduced outflow facility, and the isotype antibody control had minimal effects. Several antibodies (AAb-1–AAb-19) targeting ANGPTL7 eliminated the reduction in outflow facility ($n = 3$; $^{*}P < 0.05$, $^{**}P < 0.005$ vs. treatment with ANGPTL7 + isotype control antibody, ANOVA with Holm–Sidak's multiple comparison test). Data are shown as mean ± SEM.

S3A). These results suggest that the majority of ANGPTL7 is generated by the TM and drains via the outflow tract.

Guided by the functional testing in our bioengineered 3D-HTM/HSC model and the measurements of ANGPTL7 levels ex vivo, we tested our top antibodies in two complementary models: perfused human globes to evaluate the effects on outflow facility and rabbits to determine the durability of the IOP effects. To test the functionality of ANGPTL7 IgGs in the aqueous outflow pathway, we perfused six pairs of human donor eyes with AAb-4 for 3 hours. Outflow facility was 58% to 88% higher at each hourly time point in the presence of AAb-4, with significance reached at hours 2 and 3 (Fig. 5B).

Next, we tested the ability of the antibodies to regulate IOP in vivo. AAb-1 was intravitreally injected into three rabbit OD eyes. Antibody buffer was used as a vehicle

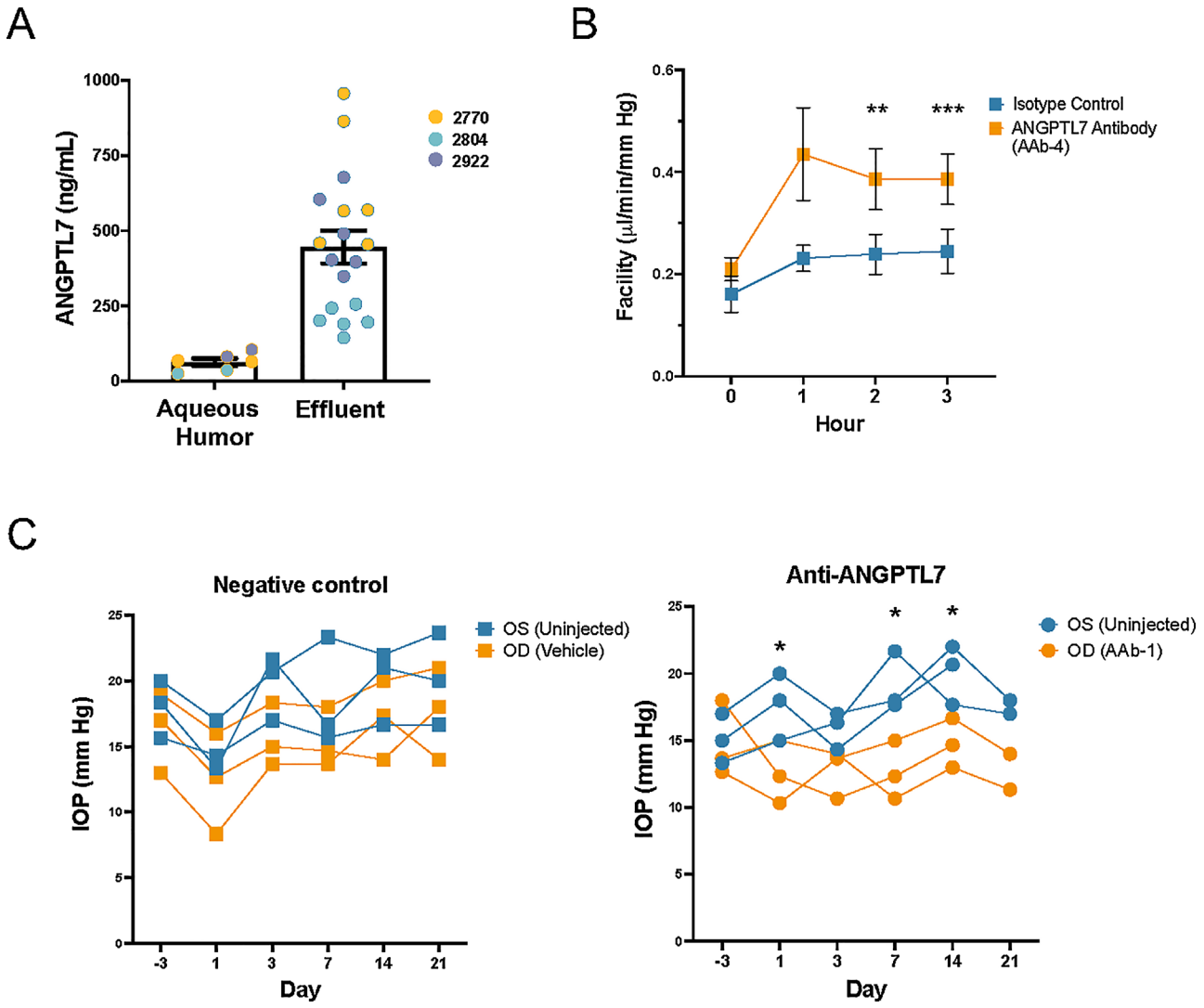

Figure 5. ANGPTL7 antibodies caused a increase in outflow facility and decrease in IOP. (**A**) Human donor eyes were placed on our custom eye mounts in a humidified and temperature-controlled water bath. Aqueous humor was extracted, and eyes were perfused. Effluent was collected over time. Three pairs of human donor eyes were perfused over 4 hours at a constant flow rate of 2.5 µL/min while pressure was continuously monitored to calculate outflow facility. Effluent was collected hourly. ANGPTL7 levels were dramatically higher in the effluent (445.6 ± 232.0 ng/mL; $n = 18$) than the aqueous humor (63.5 ± 29.2 ng/mL; $n = 6$; $P = 0.0007$, unpaired *t*-test). The three patients are indicated in *different colors*. No significant changes were seen across time points. (**B**) Outflow facility, reported as isotype IgG versus anti-ANGPTL7 IgG (AAb-4), in human eyes ($n = 6$ pairs) perfused with anti-ANGPTL7 IgG at a constant pressure of 15 mmHg showed a 61% increase in facility at 2 hours (0.24 ± 0.10 vs. 0.39 ± 0.15 µL/min/mmHg, $^{**}P = 0.0011$) and a 58% increase at 3 hours (0.24 ± 0.10 vs. 0.39 ± 0.12 µL/min/mmHg, $^{***}P < 0.0001$), with 1 hour trending toward an increase in facility (0.23 ± 0. 06 vs. 0.43 ± 0 .22 µL/min/mmHg, an 88% increase; $P = 0.058$). Statistical significance was determined by paired *t*-test. (**C**) New Zealand White rabbits were intravitreally injected with 2 mg of an antibody targeting ANGPTL7 (AAb-1) or a vehicle control in the OD eye, and IOP was measured over 21 days. Percent reduction in IOP was calculated compared to the contralateral non-injected OS eye ($n = 3$ eyes at each time point, except for $n = 2$ on day 21 for AAb-1 after one rabbit was removed on day 18 out of an abundance of caution due to slight squinting of the OD eye). Data are shown as mean ± SD.

control and was injected into three separate OD eyes. No OS eyes were injected. IOP was lower in the AAb-1-injected eyes compared to the vehicle-injected eyes (Fig. 5C, Supplementary Fig. S3B), indicating that the antibodies are functional in vivo.

Discussion

In this study, we provide new insights into the role of ANGPTL7 in IOP regulation and glaucoma. We found that deletion of *Angptl7* in mice slightly elevated baseline IOP but not outflow facility. However, these *Angptl7* KO mice displayed an impaired response to Dex, which had not been observed before except in mice overexpressing the glucocorticoid-beta receptor.[22] We further showed that glucocorticoids increased *ANGPTL7* expression in TM cells and increased ANGPTL7 levels in human aqueous humor. Taken together, these data suggest that ANGPTL7 is a key player in steroid-induced ocular hypertension.

Expression of both the *ANGPTL7* gene and ANGPTL7 protein was consistently induced by steroids across primary HTM cell strains derived from four different eye donors. In

aqueous humor, we found that increased ANGPTL7 correlated with steroid treatment, regardless of whether the patient was diagnosed with glaucoma. A previous study found elevated levels of ANGPTL7 in glaucoma patients compared to control[8]; however, we encountered many glaucoma patients with ANGPTL7 levels below the detection limit of ELISA, thereby nudging the mean of glaucoma patients not treated with steroids to be similar to that of controls. With a more sensitive assay, we might see greater separation between control and glaucoma patients. It is possible that ANGPTL7 could be more highly elevated according to the type of glaucoma, severity of disease, or time since diagnosis. The dataset was also complicated by the inclusion of a number of uveitic glaucoma patients. Thus, we were unable to perform these subgroup analyses due to the size of our dataset. It is also unclear how other glaucoma therapies affect ANGPTL7 levels, as nearly all of the patients were receiving at least one line of treatment and/or had an IOP-reducing ocular procedure in our cohort.

With the goal of therapeutically blocking the activity of ANGPTL7 in the aqueous humor in patients with glaucoma, we generated antibodies targeting ANGPTL7. These antibodies were screened in a co-culture assay of TM and SC cells that was finely tuned to the level of ANGPTL7 that significantly reduced hydraulic conductivity. The globular fibrinogen domain is considered to be responsible for functional interactions, whereas the stalk drives formation of the multimer. Peptide scanning mapping of the epitopes recognized by the blocking antibodies indicated that they recognize overlapping regions of the fibrinogen domain, suggesting that this domain is important for regulation of IOP by ANGPTL7. In addition to their therapeutic potential, these antibodies will be important tools to determine the mechanism by which ANGPTL7 acts on the aqueous outflow pathway to regulate IOP, as we have shown that inhibition of ANGPTL7 using our therapeutic antibodies increases outflow facility. Importantly, functional validation of our top candidate, which was identified in our antibody screening assay, demonstrated an efficacious and durable lowering of IOP when injected intravitreally into rabbit eyes. Although the absence of an isotype antibody in the control group is a limitation, this result is consistent with data showing that single nucleotide polymorphisms (SNPs) in *ANGPTL7* that protect against the risk of elevated IOP and glaucoma decrease secreted ANGPTL7.[4,7]

To examine the role of ANGPTL7 in IOP homeostasis, we examined mice with depleted amounts of Angptl7. In the setting of a healthy young mouse, we detected a significant increase in baseline IOPs between WT and *Angptl7* KO mice at two different locations. Although the absolute IOPs varied between the two locations, the pattern remained the same. IOP variation can be caused by differences in vivarium environmental conditions and by operator and technique.[23,24] IOPs at both sites were measured within a few minutes of sedation to reduce the impact on IOP.

Interestingly, our mouse results differed from those of another group who recently showed that IOP was significantly *lower* in *Angptl7* KO mice.[4] It is important to note that the two KO mouse lines were generated by different mechanisms of *Angptl7* gene deletion and were on different genetic backgrounds, all of which can contribute to differing IOP results. Similar paradoxical effects on IOP have been observed in other KO mice on different backgrounds.[25]

Although there is evidence of the role of ANGPTL7 in IOP regulation, the precise mechanism guiding these effects remains under investigation. It has been suggested that ANGPTL7 alters the expression levels of genes and proteins associated with the extracellular matrix (ECM).[9] These in vitro data from cells grown on a monolayer are consistent with our results indicating that excess of ANGPTL7 causes an increase in IOP, and knockout of *Angptl7* confers protection against steroid-induced ocular hypertension, as steroids induce ECM expression. However, this hypothesis is not consistent with the immediate effects of our ANGPTL7 blocking antibody perfused into human donor eyes, where we observed a rapid and robust increase in outflow facility. As well, we did not see demonstrable changes in expression of a subset of ECM genes previously shown to be altered with treatment of ANGPTL7 in 3D HTM cell culture (data not shown). As a more unbiased approach, we performed RNA sequencing experiments on primary HTM and HSC cells treated with ANGPTL7 and grown as both monolayer cultures and as a co-culture, and both experiments yielded no genes with significantly changed expression levels (not shown). We surmise that ANGTPL7 exerts its effect via interactions at the protein level as evidenced by the rapid and robust effect of anti-ANGPL7 antibodies on outflow facility in human eyes. Although further investigation into the mechanism of action of ANGPTL7 is necessary, evidence from multiple model systems and patients with protective SNPs indicates that lowering ANGPTL7 levels is a viable therapeutic strategy for lowering IOP in POAG.

Acknowledgments

Human aqueous humor samples were provided by the University of California, San Francisco, courtesy of Jay Stewart, Ricardo Lamy, Joshua Wu, and Daphne Yang.

Supported by grants from the National Institutes of Health (EY022359, EY005722) and by an unrestricted grant from Research to Prevent Blindness Foundation.

Disclosure: **S.F.-K. Brown**, Broadwing Bio (E); **H. Nguyen**, Broadwing Bio (E); **P. Mzyk**, None; **M.L. De Ieso**, None; **A.M. Unser**, Humonix Biosciences (E); **I. Brown**, Broadwing Bio (E); **P. Ramesh**, Humonix Biosciences (E); **H. Afzaal**, Humonix Biosciences (E); **F. Ahmed**, Humonix Biosciences (E); **K.Y. Torrejon**, Humonix Biosciences (E); **A. Nhan**, Alloy Therapeutics (E); **D. Markrush**, Alloy Therapeutics (E); **T. Daly**, Alloy Therapeutics (E); **E. Knecht**, Alloy Therapeutics (E); **W. McConaughy**, Alloy Therapeutics (E); **S. Halmos**, Alloy Therapeutics (E); **Z.L. Liu**, Alloy Therapeutics (E); **R. Rennard**, Alloy Therapeutics (E); **A. Peterson**, Broadwing Bio (E), 82VS (C); **W.D. Stamer**, Broadwing Bio (C, F)

References

1. Flaxman SR, Bourne RRA, Resnikoff S, et al. Global causes of blindness and distance vision impairment 1990–2020: a systematic review and meta-analysis. *Lancet Glob Health*. 2017;5:e1221–e1234.
2. Kang JM, Tanna AP. Glaucoma. *Med Clin North Am*. 2021;105:493–510.
3. Tanigawa Y, Wainberg M, Karjalainen J, et al. Rare protein-altering variants in *ANGPTL7* lower intraocular pressure and protect against glaucoma. *PLoS Genet*. 2020;16:e1008682.
4. Praveen K, Patel GC, Gurski L, et al. *ANGPTL7*, a therapeutic target for increased intraocular pressure and glaucoma. *Commun Biol*. 2022;5:1051.
5. Rozsa FW, Reed DM, Scott KM, et al. Gene expression profile of human trabecular meshwork cells in response to long-term dexamethasone exposure. *Mol Vis*. 2006;12:125–141.

6. Voigt AP, Whitmore SS, Lessing ND, et al. Spectacle: an interactive resource for ocular single-cell RNA sequencing data analysis. *Exp Eye Res*. 2020;200:108204.
7. Aboobakar IF, Collantes ERA, Hauser MA, Stamer WD, Wiggs JL. Rare protective variants and glaucoma-relevant cell stressors modulate *Angiopoietin-like 7* expression. *Hum Mol Genet*. 2023;32:2523–2531.
8. Kuchtey J, Källberg ME, Gelatt KN, Rinkoski T, Komàromy AM, Kuchtey RW. Angiopoietin-like 7 secretion is induced by glaucoma stimuli and its concentration is elevated in glaucomatous aqueous humor. *Invest Ophthalmol Vis Sci*. 2008;49:3438–3448.
9. Comes N, Buie LK, Borrás T. Evidence for a role of angiopoietin-like 7 (ANGPTL7) in extracellular matrix formation of the human trabecular meshwork: implications for glaucoma. *Genes Cells*. 2011;16:243–259.
10. Zhao X, Ramsey KE, Stephan DA, Russell P. Gene and protein expression changes in human trabecular meshwork cells treated with transforming growth factor-β. *Invest Ophthalmol Vis Sci*. 2004;45:4023–4034.
11. Santulli G. Angiopoietin-like proteins: a comprehensive look. *Front Endocrinol (Lausanne)*. 2014;5:4.
12. Gur-Cohen S, Yang H, Baksh SC, et al. Stem cell-driven lymphatic remodeling coordinates tissue regeneration. *Science*. 2019;366:1218–1225.
13. De Ieso ML, Kelly R, Mzyk P, Stamer WD. Development and testing of a metabolic chamber for effluent collection during whole eye perfusions. *Exp Eye Res*. 2023;236:109652.
14. Keller KE, Bhattacharya SK, Borrás T, et al. Consensus recommendations for trabecular meshwork cell isolation, characterization and culture. *Exp Eye Res*. 2018;171:164–173.
15. Stamer WD, Seftor RE, Williams SK, Samaha HA, Snyder RW. Isolation and culture of human trabecular meshwork cells by extracellular matrix digestion. *Curr Eye Res*. 1995;14:611–617.
16. Stamer WD, Clark AF. The many faces of the trabecular meshwork cell. *Exp Eye Res*. 2017;158:112–123.
17. Bastia E, Toris CB, Brambilla S, et al. NCX 667, a novel nitric oxide donor, lowers intraocular pressure in rabbits, dogs, and non-human primates and enhances TGFβ2-induced outflow in HTM/HSC constructs. *Invest Ophthalmol Vis Sci*. 2021;62:17.
18. Torrejon KY, Pu D, Bergkvist M, Danias J, Sharfstein ST, Xie Y. Recreating a human trabecular meshwork outflow system on microfabricated porous structures. *Biotechnol Bioeng*. 2013;110:3205–3218.
19. Geysen HM, Meloen RH, Barteling SJ. Use of peptide synthesis to probe viral antigens for epitopes to a resolution of a single amino acid. *Proc Natl Acad Sci USA*. 1984;81:3998–4002.
20. Timmerman P, Puijk WC, Meloen RH. Functional reconstruction and synthetic mimicry of a conformational epitope using CLIPS technology. *J Mol Recognit*. 2007;20:283–299.
21. Overby DR, Bertrand J, Tektas OY, et al. Ultrastructural changes associated with dexamethasone-induced ocular hypertension in mice. *Invest Ophthalmol Vis Sci*. 2014;55:4922–4933.
22. Patel GC, Liu Y, Millar JC, Clark AF. Glucocorticoid receptor GRβ regulates glucocorticoid-induced ocular hypertension in mice. *Sci Rep*. 2018;8:862.
23. Li L, Zhou J, Fan W, et al. Lifetime exposure of ambient $PM_{2.5}$ elevates intraocular pressure in young mice. *Ecotoxicol Environ Saf*. 2021;228:112963.
24. Reina-Torres E, Bertrand JA, O'Callaghan J, Sherwood JM, Humphries P, Overby DR. Reduced humidity experienced by mice in vivo coincides with reduced outflow facility measured ex vivo. *Exp Eye Res*. 2019;186:107745.
25. Suarez MF, Schmitt HM, Kuhn MS, et al. Genetic background determines severity of Loxl1-mediated systemic and ocular elastosis in mice. *Dis Model Mech*. 2023;16:dmm050392.

Investigative Ophthalmology & Visual Science